

# Oil & Natural Gas Technology

DOE Award No.: DE-FC26-06NT43067

## Quarterly Progress Report (April - June 2010)

### Mechanisms Leading to Co-Existence of Gas and Hydrate in Ocean Sediments

Submitted by:  
The University of Texas at Austin  
1 University Station C0300  
Austin, TX 78712-0228

Prepared for:  
United States Department of Energy  
National Energy Technology Laboratory

August 23, 2010



Office of Fossil Energy

MECHANISMS LEADING TO CO-EXISTENCE OF GAS AND HYDRATE IN  
OCEAN SEDIMENTS

CONTRACT NO. DE-FC26-06NT43067

**QUARTERLY PROGRESS REPORT**  
**Reporting Period: 1 Apr 10 –30 Jun 10**

*Prepared by*

**Steven L. Bryant**

Department of Petroleum and Geosystems Engineering  
The University of Texas at Austin  
1 University Station C0300  
Austin, TX 78712-0228  
Phone: (512) 471 3250  
Email: steven\_bryant@mail.utexas.edu

**Ruben Juanes**

Department of Civil and Environmental Engineering  
Massachusetts Institute of Technology  
77 Massachusetts Avenue, Room 48-319  
Cambridge, MA 02139  
Phone: (617)253-7191  
Email: juanes@mit.edu

*Prepared for*

**U.S. Department of Energy - NETL**  
3610 Collins Ferry Road  
P.O. Box 880  
Morgantown, WV 26508

Acknowledgment: "This material is based upon work supported by the Department of Energy under Award Number DE-FC26-06NT43067."

Disclaimer: "This report was prepared as an account of work sponsored by an agency of the United States Government. Neither the United States Government nor any agency thereof, nor any of their employees, makes any warranty, express or implied, or assumes any legal liability or responsibility for the accuracy, completeness, or usefulness of any information, apparatus, product, or process disclosed, or represents that its use would not infringe privately owned rights. Reference herein to any specific commercial product, process, or service by trade name, trademark, manufacturer, or otherwise does not necessarily constitute or imply its endorsement, recommendation, or favoring by the United States Government or any agency thereof. The views and opinions of authors expressed herein do not necessarily state or reflect those of the United States Government or any agency thereof."

## **Summary**

Work during this period has focused on the analysis of the bed-scale model for development of hydrate in sub-permafrost environments. During this reporting period, we presented this work at several venues<sup>1</sup>.

The description of the model in this report has been refined so as to highlight the roles of the five essential elements of the model:

1. An existing gas column converts to hydrate as BGHSZ descends
2. Element (1) causes movement of fluid phase(s) toward hydrate-forming region
3. Element (2) causes reduction in gas capillary pressure throughout the gas column
4. Element (3) combined with sedimentological heterogeneity leads to disconnection(s) within the gas column
5. Elements (2) and (4) lead to sandwich-like distribution of hydrate saturation with depth

This simple model provides a mechanistic explanation for the observation of layers of small but nonzero hydrate saturations between layers bearing large saturation -- even when the layers are in sand-rich sediments. Indeed, even an initially uniform distribution of gas saturation will yield a non-uniform hydrate saturation under this model. Wells in the North American Arctic (Mt. Elbert, Alaska and Mallik, NW Territories) exhibit such hydrate distributions.

The model makes other testable predictions. One is that the vertical extent of the initial gas column is the same as the vertical extent of the final hydrate distribution. In this sense the model can be run backwards to predict the original gas saturation distribution from the currently observed hydrate saturation distribution. This prediction can be tested against understanding from classical hydrocarbon systems, for example, whether the predicted original gas saturation is consistent with a spill point, seal quality, availability of charge, etc. Another prediction is that sandwich-like hydrate distribution requires capillary barriers within the sediment column of sufficient strength to disconnect the gas column but not so strong as to prevent establishing the initially continuous column. Such barriers are evident at Mt. Elbert, but only half of the barriers needed are evident from available data for Mallik. The implications of the latter observation are still being investigated.

---

<sup>1</sup> 2009 AGU Fall Meeting: 14-18 December, San Francisco;  
NETL Hydrate meeting: January 25-28, 2010, Atlanta;  
2010 AAPG conference: 11<sup>th</sup>-14<sup>th</sup> April, New Orleans;  
Gordon Research conference: Natural Gas Hydrate Systems, June 6-11, 2010, Waterville, ME

## ***Activities in This Reporting Period***

### **Task 8.0 - Modeling methane transport at the bed scale**

#### ***Influence of sedimentological heterogeneity on hydrate saturation as BGHSZ descends through a gas accumulation***

For completeness we summarize the conceptual model, various aspects of which have also been described in recent progress reports. We then point out some important implications of the model, and show how they can be tested against field measurements.

#### **Conceptual Model**

The underlying model assumption is that a gas column has accumulated beneath a conventional petroleum trap in the Arctic. The accumulation is assumed to have occurred while the base of the gas hydrate stability zone (BGHSZ) is far above the seal of the trap. The accumulation is assumed to be disconnected from the original source of gas charge by the time the BGHSZ begins to descend through the accumulation.

The saturation of the gas phase in the accumulation, Figure 1, can vary with depth as the grain size distribution in the sediment varies. Likewise the capillary entry pressure varies with depth -- this is the source of sedimentological control on hydrate distribution. As BGHSZ falls (Figure 2), the accumulated gas and water are converted to hydrate.

Crucially, the conversion to hydrate reduces the volume occupied by gas and water molecules, Figure 3. This is because the density of CH<sub>4</sub> molecules in the gas phase at conditions typical of subpermafrost ( $T \sim 5^\circ\text{C}$ ,  $P \sim 7 \text{ MPa}$ ,  $\rho_g \sim 50 \text{ kg/m}^3$ ) is considerably less than the density of CH<sub>4</sub> molecules in the hydrate phase ( $\rho_h \sim 118 \text{ kg CH}_4/\text{m}^3 \text{ hydrate}$ ). In the subsurface, this means that the gaseous and/or aqueous phases will move toward the BGHSZ to fill the void that would otherwise occur as hydrate forms.

The movement of fluid phases required by hydrate formation has important implications. For a gas accumulation no longer connected to the source of gas charge, the gas-water contact (GWC) will rise as hydrate forms at the top of the accumulation, Fig. 4(a). As the GWC rises, a zone of residual gas saturation is established in the lower portion of the gas accumulation, Fig. 4(b). The conversion of the smaller residual gas saturation to hydrate yields a significantly smaller hydrate saturation, Fig. 4(c). Hence even an initially uniform distribution of gas saturation is converted to a nonuniform hydrate saturation distribution.

#### **Model Implications: Sandwich-like hydrate saturation profiles**

Another effect of the rising GWC is that the capillary pressure throughout the gas column decreases. This is because the gas phase at residual saturation is by definition disconnected. Thus the gas phase pressure increases from hydrostatic only above the

transition from residual saturation to original saturation. This behavior is illustrated in Figure 5 using sedimentological data for the Mt. Elbert well. The GWC at time  $t_0$  is at an assumed gas charge location, here assumed to be at a depth of 759 m. (This value is chosen for illustration. Any geologically plausible value could be used, the effect being to change the height of the initial gas accumulation.) The GWC rises to depth 741 m at time  $t_1$ , in response to gas moving upward within the accumulation as hydrate forms at the top of the accumulation. Consequently the capillary pressure in the gas phase follows the solid blue line at time  $t_1$ , an upwards shift of the original  $P_c$  vs.  $z$  trend (dashed blue line).

Of particular interest at time  $t_1$  is that the gas capillary pressure becomes equal to the capillary entry pressure at a depth of 735 m (green oval in Figure 5). Thus when more hydrate forms as the BGHSZ moves down, *the upward moving gas will disconnect itself* at a depth of 735 m. That is, the next incremental upward shift of the  $P_c$  vs.  $z$  line will reduce the capillary pressure at 735 m to a value below the entry pressure for the sediment at that depth. The (short) gas column below this depth thus becomes disconnected from the gas column above 735 m. Continued hydrate formation will continue to draw gas upward, but now only from the gas column held between 615 and 735 m. In effect, as shown in Figure 6, we now have two GWC, one at depth 735 and another at depth 740 m. The one at 740 m remains fixed until the BGHSZ falls to that depth. The one at 735 m rises as hydrate forms at the BGHSZ until the upward-shifting  $P_c$  vs  $z$  trend crosses the next peak in the capillary entry pressure. This occurs at time  $t_2$  in Figure 6. As this process continues, the original continuous gas column is broken into a series of thin, isolated "mini-accumulations", Figure. 7. Each "mini-accumulation" behaves just like the single accumulation in Figure 4 as BGHSZ descends. Thus each "mini-accumulation" is converted into a layer with large hydrate saturation in the upper portion and small hydrate saturation in the lower portion, Figure 8.

Ultimately, after the BGHSZ has descended through the entire gas column, Figure 9, we see the consequence of sedimentological heterogeneity (here, variation in grain size distribution with depth): the initially uniform gas saturation is converted to a sandwich-like profile of large and small -- but never zero-- hydrate saturations.

### **Model Implications: Influence of initial gas charge on hydrate distribution**

We remark that this model can be used in a diagnostic fashion to infer the original gas column height from modern observation of hydrate saturation distribution. The model results in Figures 5-9 assumed a large initial gas column, from 759 m to 615 m, and yields nonzero gas hydrate saturations across the same interval. However, the Mt. Elbert well, from which the capillary entry pressure profile in Figures 5-9 was inferred, only shows nonzero hydrate saturation (as inferred from well log responses) between depths of 675 m and 615 m. If our conceptual model is valid, then it must be the case that the initial gas column only extended from 675 m to 615 m. If we make this assumption and then apply the same procedure as illustrated in Figures 5-9, we predict the hydrate saturation profile shown in Figure 10. (The parameter  $R$ , here set to 0.1, refers to a nominal

"mobility ratio", which is equivalent to the fraction of water that moves to the BGHSZ relative to the total amount of gas and water that moves. The physical basis of this parameter will be described in future reports.) The agreement between the model and the observations in Figure 10 is good. *Importantly, the model provides a mechanistic explanation for the otherwise quite puzzling observation of small (but not zero) hydrate saturation in the interval between 630 m and 650 m depth.*

The prediction that the original gas accumulation extended from 615 m to 675 m depth can be tested against understanding derived from conventional petroleum systems analysis. For example, the seal at 615 m is required to hold a 60 m column of gas. The conventional estimate of entry pressure from the grain size distribution, Figure 5, suggests that the seal would have held about 15 to 20 m of gas column. It is conceivable that the fining-upwards trend that is evident between 617 and 615 m continues above 615 m, yielding a stronger capillary barrier, i.e. grain sizes about 3 times smaller than those at 615 m. Unfortunately about 1.5 m of core immediately above 615 m was not recovered, so it is not possible to test this possible explanation further.

The preceding analysis of seal capacity leads to another line of investigation. If the seal were capable of holding no more than 60 m of gas column, then the establishment of the initial gas column would have been limited to 60 m. If the seal were capable of holding more than 60 m of gas column, then we would need to explain why only 60 m was apparently established. This would involve analysis of spill points and the timing of the gas charge. In the case of Mt. Elbert the question has been raised, at least anecdotally, as to whether partial gas charge can explain the heterogeneous distribution of hydrate saturation. The model suggests that nonuniform hydrate saturations are inevitable, regardless of the extent of charge. This argues that main influence of partial charge would be on the height of the initial gas column and hence upon the overall thickness of the hydrate accumulation. The broader analysis of charge, seal capacity etc. is beyond the scope of the project. Nevertheless our intention in the remainder of the project is to seek at least qualitative evidence that would help confirm or refute the model.

We include these still speculative considerations in this report to highlight the fact that model is mechanistic and can be tested more rigorously with petroleum systems analysis. This lays a foundation for future work on this class of hydrate accumulation. We also remark that nonuniform distributions of hydrate saturation have been reported from the Gulf of Mexico JIP wells and even in some ocean sediments. It may be instructive to revise the Arctic model for application to these provinces if the basis for moving the BGHSZ is, for example, a change in sea level.

### **Model Implications: Influence of quality of local capillary seals on hydrate distribution**

We have applied the model, which works well for Mt. Elbert, to the geologically analogous accumulation of hydrate in the Mallik well. We assume plentiful gas charge so that the initial gas saturation profile is determined by the capillary barriers distributed through the sediment column. The barriers correspond to local minima in the mean grain

size distribution, Figure 12 (a)-(b). None of the barriers are capable of supporting a gas column higher than 20 m. Thus the initial saturation profile consists of large saturations just below each barrier, Figure 12(c). The large saturations extend only to a depth corresponding to the column height supportable by each barrier. Below each column of large gas saturation is an interval of small gas saturation. This saturation would correspond to the critical gas saturation (the saturation needed for gas to flow through the porous medium), assumed to be 30% in this example. With these assumptions, the model yields the hydrate saturation profile of Figure 12(d). The predicted hydrate distribution (green line) does not agree with the observations. Either the model of hydrate formation is not applicable at Mallik, or the assumed conditions for the establishing the initial saturation distribution are wrong.

Since the model seems to work well for Mt. Elbert and it is likely that Mallik experienced the same history for the depth of BGHSZ, we tentatively conclude that the presumed initial gas saturation distribution is incorrect. It is instructive to consider what the initial distribution would have to be in order to yield a hydrate saturation distribution similar to that observed. Figure 12 shows the results of applying the model if strong capillary barriers are assumed to exist at depths of 941 m, 951 m, 969 m and 1005 m (red dotted lines in panels c and d of Figure 12.) In this case the model predicts hydrate distribution quite similar to the observed distribution, Figure 12(d).

This analysis raises the obvious question as to whether such barriers actually exist. Certainly a fine-grained interval exists at 941 m and 1005 m (note peak in entry pressure trend in Figure 12(b)), so a stronger barrier than estimated in Figure 11 at those locations is plausible. But the basis for invoking barriers at 951 m and 969 m is not evident from the data available. The value of visual inspection of core become apparent in this context, since thin, silty layers could lie between the points sampled for grain size analysis. The implications of this test of the model are still under investigation and will be discussed in future reports.

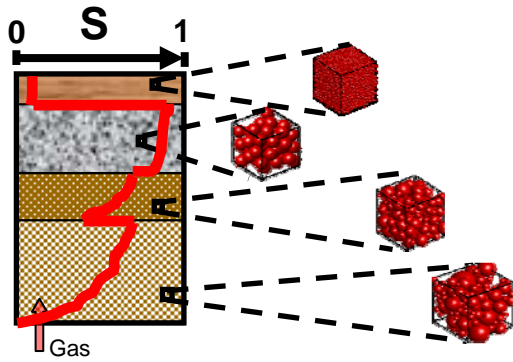


Figure 1. Rising gas accumulates below the finest-grained formation (the seal at top of package) at saturations that vary with grain size distribution.

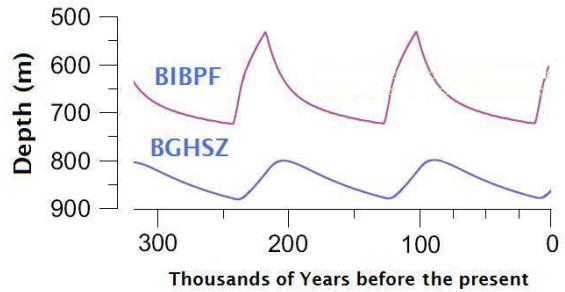


Figure 2. BGHSZ (base of gas hydrate stability zone) and BIBPF (base of ice-bearing permafrost) cycle with geological time in Alaska/Northwest Territories.

**Closed system held at constant  $T, P$  with a movable piston**

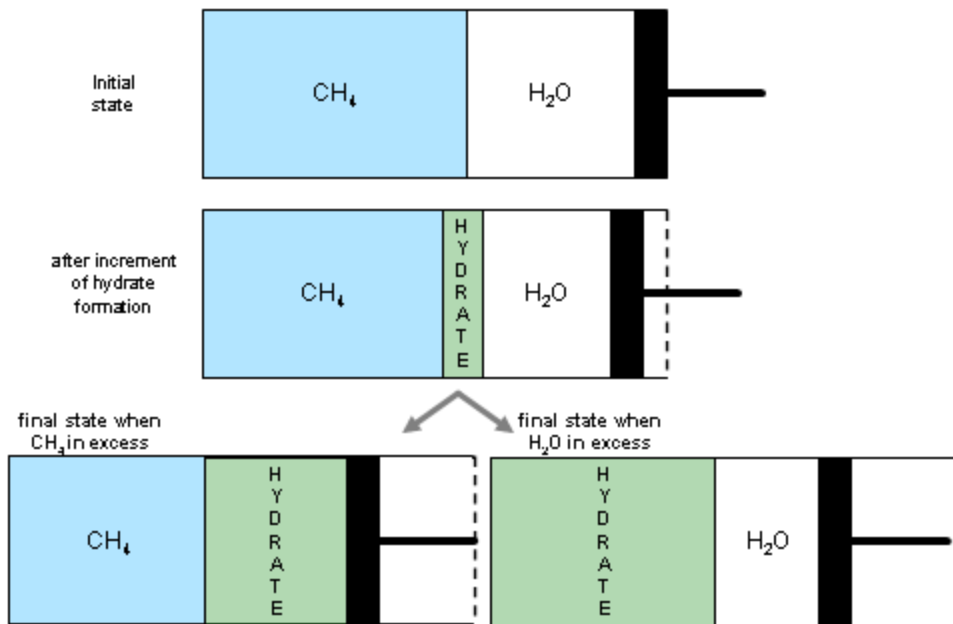


Figure 3. In a closed system, the volume occupied by gas and water phases at  $T$  and  $P$  typical of sub-permafrost formations in the Arctic exceeds the volume occupied at equilibrium, when the limiting reagent (either  $\text{CH}_4$  or  $\text{H}_2\text{O}$ ) is completely converted to hydrate. Consequently in the natural, open system, the formation of hydrate will cause one or both phases (gas, aqueous) to move into the vacated pore space.

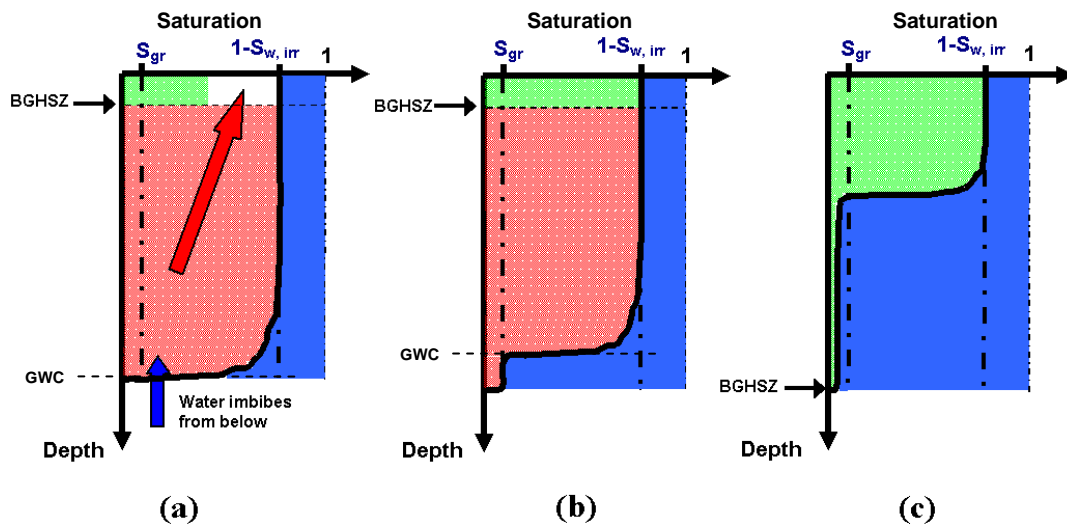


Figure 4. Schematic of the development of hydrate saturation as BGHSZ descends through an existing accumulation of gas. (a) Formation of hydrate (green) at top of gas accumulation creates a void (white) that is filled by gas (red arrow) from below and water. Water also imbibes into the bottom of the gas accumulation (blue arrow). (b) Hydrate eventually fills the top part of the gas accumulation, and the gas that has moved up to form this hydrate leaves residual saturation below the new gas water contact (GWC). (c) After BGHSZ reaches bottom of the original accumulation, the hydrate saturation is large in the upper part of the accumulation. The small hydrate saturation in the lower part of the accumulation is the result of converting residual gas to hydrate.

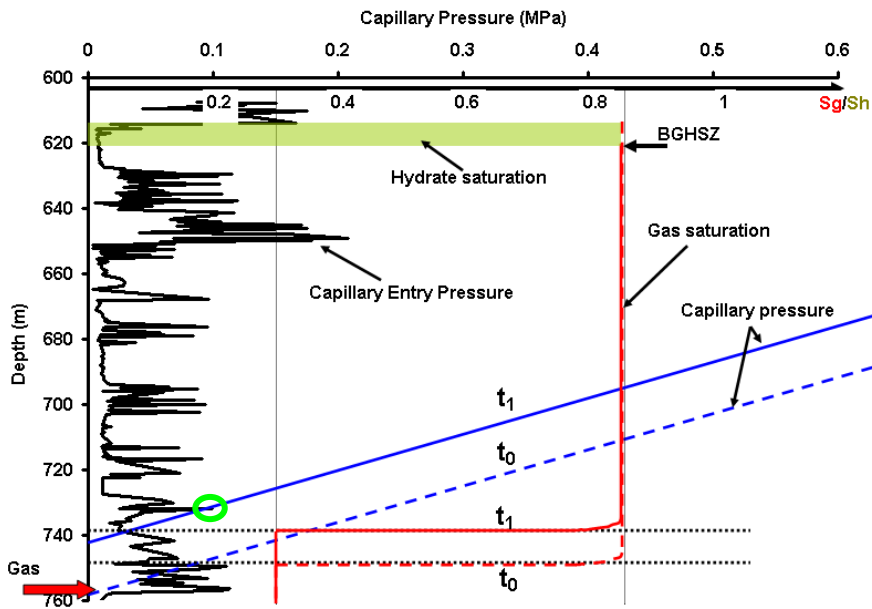


Figure 5. Gas charge, assumed to enter at a depth of 755 m, establishes a gas accumulation (dashed red curve) in a heterogeneous sediment with varying capillary entry pressure. The entry pressure values are inferred from the grain size distribution measured for the Mt. Elbert formation (data courtesy W. Winters, USGS and K. Rose, NETL). Hydrate (green band at depth 615-620 m) forms between time  $t_0$  and  $t_1$  as BGHSZ falls. This causes the gas saturation at depths below 740 m at time  $t_1$  (solid red curve) to drop from a large initial saturation (dashed red curve) at time  $t_0$  to a smaller residual saturation. The disconnected gas phase below depths of 739 m no longer contributes to the gas hydrostatic column. Consequently the gas phase capillary pressure decreases uniformly to the solid blue line at time  $t_1$ .

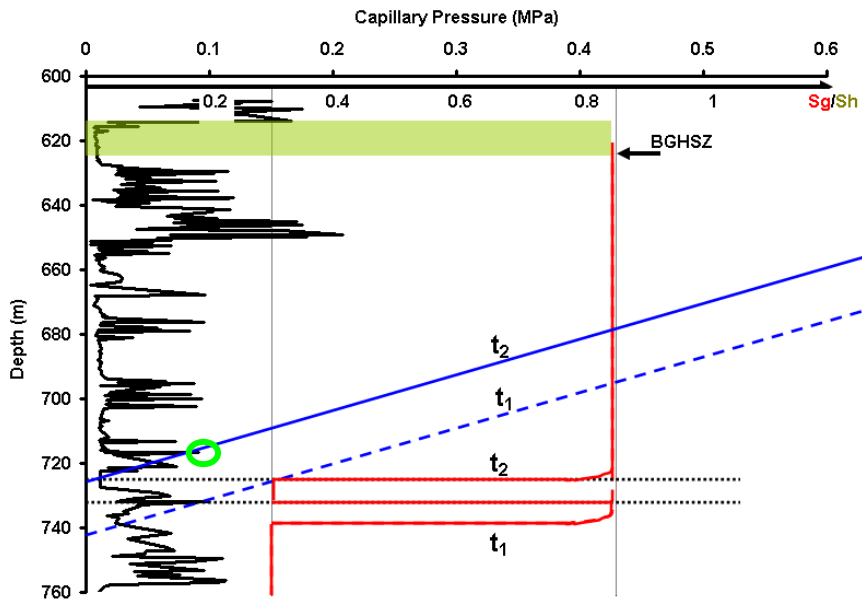


Figure 6. As BGHSZ continues to descend (cf. Figure 5), the reduction in gas phase capillary pressure (solid blue line) intersects the next peak in the plot of sediment entry pressure vs. depth. The next incremental volume of gas that rises to accommodate the incremental formation of hydrate will thus cause the gas column to be disconnected at a depth of 718 m (green oval).

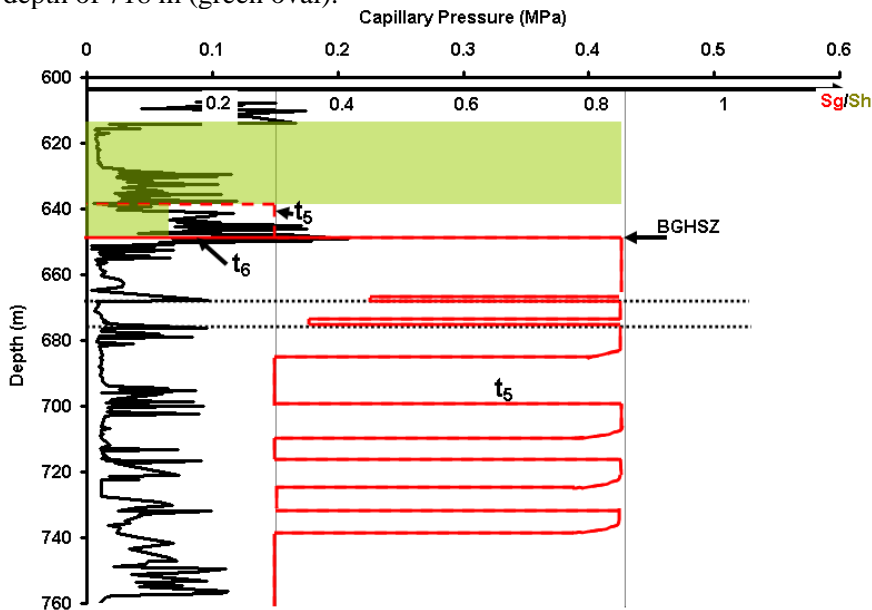


Figure 7. Continuing the process illustrated in Figures 5 and 6, the BGHSZ eventually converts the uppermost column of disconnected gas (between 615 and 647 m) into hydrate. The continued descent of BGHSZ will encounter a series of thin columns of disconnected gas, each of which has large gas saturation in the upper portion and residual gas saturation in the lower portion.

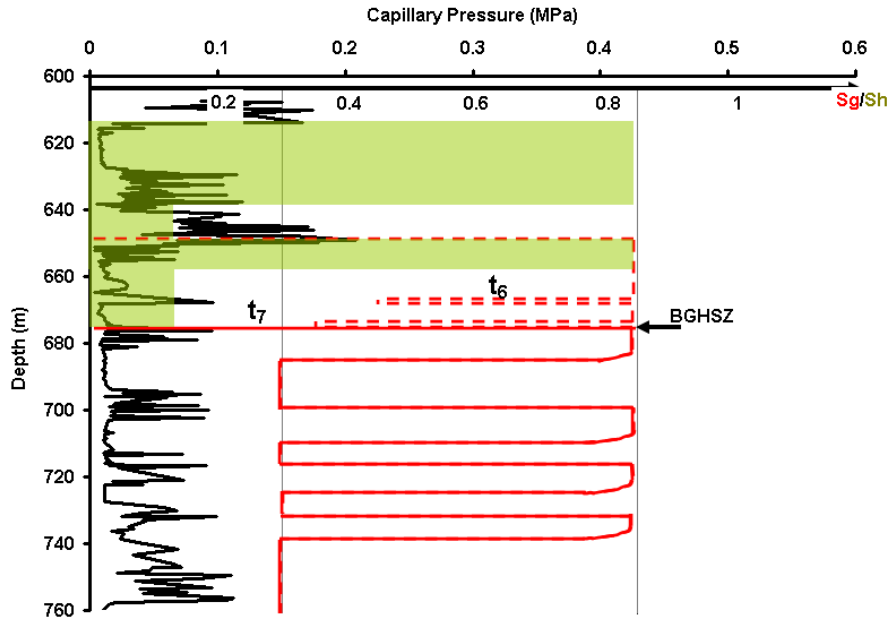


Figure 8. Continuing the process illustrated in Figure 7, the BGHSZ converts the next column of disconnected gas (between 647 and 675 m) into hydrate. The characteristic sandwich profile, in which layers of hydrate exhibit large saturation in the upper portion of the layer and small saturation in the lower portion, thus is established in this interval.

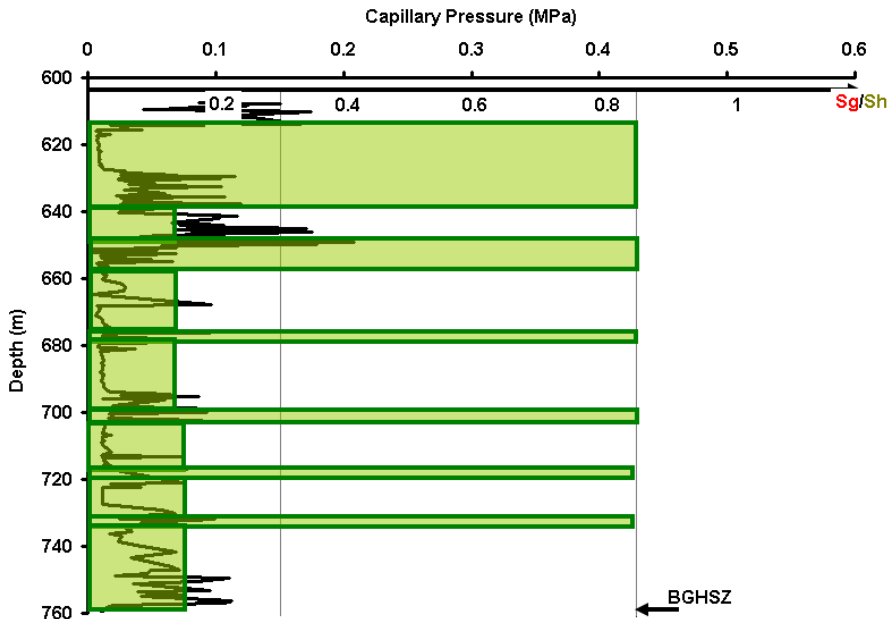


Figure 9. After the BGHSZ has descended through the entire column, the original nearly uniform gas saturation profile has been converted into a sandwich-like hydrate saturation profile.

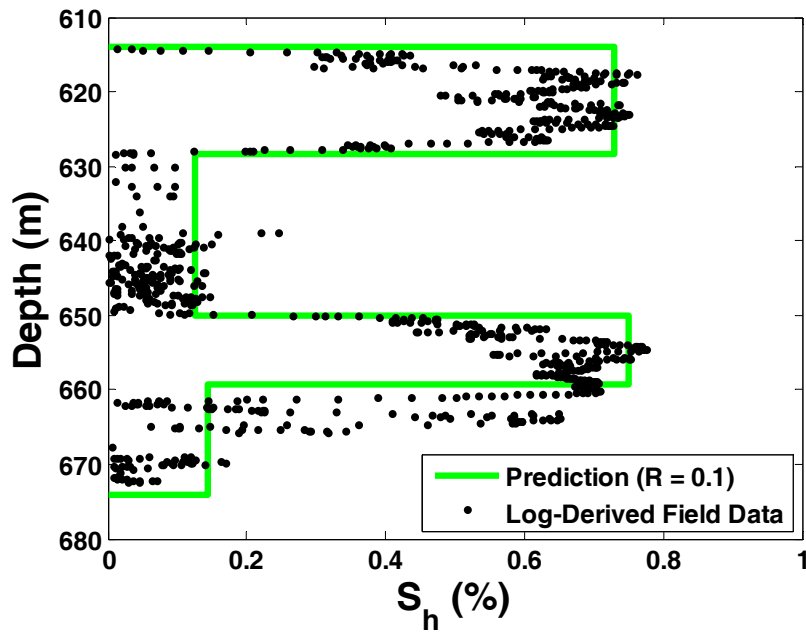


Figure 10. Application of the model to Mt Elbert formation assuming the initial gas column is limited to the interval from 615 m to 675 m. After the BGHSZ has descended through the entire column, the original nearly uniform gas saturation profile has been converted into a sandwich-like hydrate saturation profile (green line) consistent with the log-derived estimate (black dots).

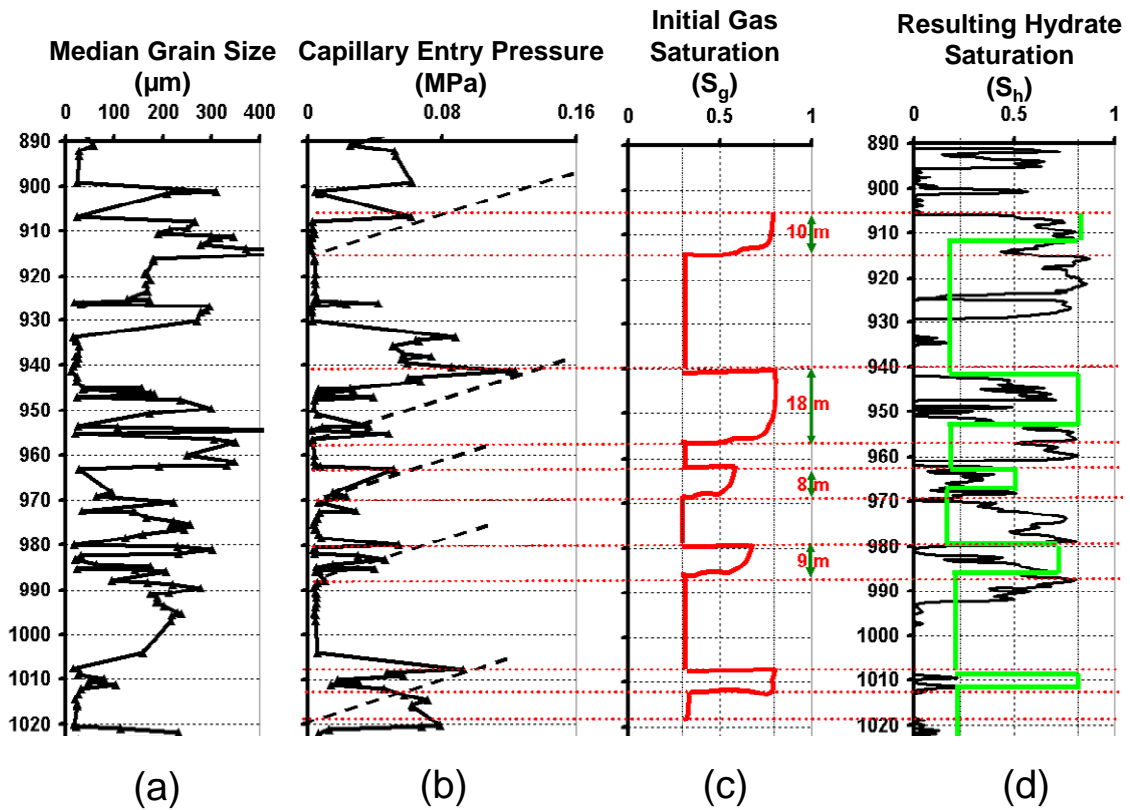


Figure 11. Application of the hydrate formation model to the Mallik well. (a) Grain size distribution reported in the literature. (b) Capillary entry pressure estimated from mean grain size. (c) A sandwich-like initial gas saturation profile is assumed between the depths of 905 m and 1015 m. The variation from large saturation to small saturation at 915 m, 958 m, 969 m, 988 m and 1013 m reflect the supportable column height beneath the corresponding local capillary seals at 905 m, 940 m, 961 m, 979 m and 1008 m. (d) After the BGHSZ has descended through the entire column, the sandwich-like gas saturation distribution is converted to a qualitatively similar sandwich-like hydrate saturation profile. The prediction is not consistent with the observation (black line)

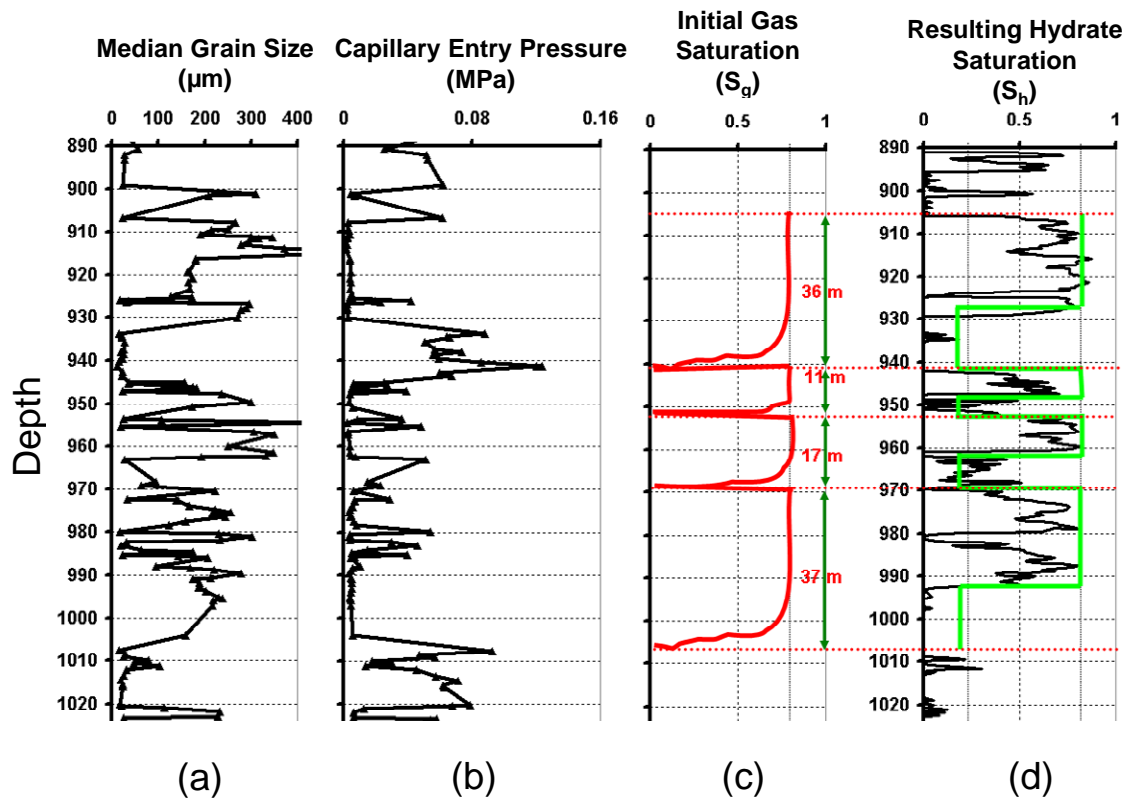


Figure 12. (a) and (b): same as Figure 11. (c) Hypothetical initial gas saturation, obtained when capillary barriers at selected locations (red dotted lines) are assumed strong enough to support the labeled gas column heights. (d) After the BGHSZ has descended through the entire column shown in panel (c), the original gas saturation profile has been converted into a sandwich-like hydrate saturation profile similar to the observed profile.

## **National Energy Technology Laboratory**

626 Cochrans Mill Road  
P.O. Box 10940  
Pittsburgh, PA 15236-0940

3610 Collins Ferry Road  
P.O. Box 880  
Morgantown, WV 26507-0880

One West Third Street, Suite 1400  
Tulsa, OK 74103-3519

1450 Queen Avenue SW  
Albany, OR 97321-2198

2175 University Ave. South  
Suite 201  
Fairbanks, AK 99709

Visit the NETL website at:  
[www.netl.doe.gov](http://www.netl.doe.gov)

Customer Service:  
1-800-553-7681

